REPORT DOCUMENTATION PAGE

Form Approved OMB NO. 0704-0188

The public reporting burden for this collection of information is estimated to average 1 hour per response, including the time for reviewing instructions, searching existing data sources, gathering and maintaining the data needed, and completing and reviewing the collection of information. Send comments regarding this burden estimate or any other aspect of this collection of information, including suggesstions for reducing this burden, to Washington Headquarters Services, Directorate for Information Operations and Reports, 1215 Jefferson Davis Highway, Suite 1204, Arlington VA, 22202-4302. Respondents should be aware that notwithstanding any other provision of law, no person shall be subject to any oenalty for failing to comply with a collection of information if it does not display a currently valid OMB control number.
PLEASE DO NOT RETURN YOUR FORM TO THE ABOVE ADDRESS.

1. REPORT DATE (DD-MM-YYYY)	2. REPORT TYPE	3. DATES COVERED (From - To)
	New Reprint	-

4. TITLE AND SUBTITLE
Development of a Finite Element Model for Blast Brain Injury and the Effects of CSF Cavitation

5a. CONTRACT NUMBER
W911NF-10-1-0526

5b. GRANT NUMBER

5c. PROGRAM ELEMENT NUMBER
611103

6. AUTHORS
Matthew B. Panzer, Barry S. Myers, Bruce P. Capehart, Cameron R. Bass

5d. PROJECT NUMBER

5e. TASK NUMBER

5f. WORK UNIT NUMBER

7. PERFORMING ORGANIZATION NAMES AND ADDRESSES
University of Pennsylvania
Office of Research Services
University of Pennsylvania
Philadelphia, PA 19104 -

8. PERFORMING ORGANIZATION REPORT NUMBER

9. SPONSORING/MONITORING AGENCY NAME(S) AND ADDRESS(ES)
U.S. Army Research Office
P.O. Box 12211
Research Triangle Park, NC 27709-2211

10. SPONSOR/MONITOR'S ACRONYM(S)
ARO

11. SPONSOR/MONITOR'S REPORT NUMBER(S)
58155-LS-MUR.14

12. DISTRIBUTION AVAILIBILITY STATEMENT
Approved for public release; distribution is unlimited.

13. SUPPLEMENTARY NOTES
The views, opinions and/or findings contained in this report are those of the author(s) and should not contrued as an official Department of the Army position, policy or decision, unless so designated by other documentation.

14. ABSTRACT
Blast-related traumatic brain injury is the most prevalent injury for combat personnel seen in the current conflicts in Iraq and Afghanistan, yet as a research community, we still do not fully understand the detailed etiology and pathology of this injury. Finite element (FE) modeling is well suited for studying the mechanical response of the head and brain to blast loading. This paper details the development of a FE head and brain model for blast simulation by examining both the dilatational and deviatoric response of the brain as potential injury mechanisms.

15. SUBJECT TERMS
Finite element model, Blast overpressure, Blast injury, Traumatic brain injury, Injury mechanism,CSF cavitation

16. SECURITY CLASSIFICATION OF:			17. LIMITATION OF ABSTRACT	15. NUMBER OF PAGES	19a. NAME OF RESPONSIBLE PERSON
a. REPORT	b. ABSTRACT	c. THIS PAGE			David Meaney
UU	UU	UU	UU		19b. TELEPHONE NUMBER: 215-573-2726

Report Title

Development of a Finite Element Model for Blast Brain Injury and the Effects of CSF Cavitation

ABSTRACT

Blast-related traumatic brain injury is the most prevalent injury for combat personnel seen in the current conflicts in Iraq and Afghanistan, yet as a research community, we still do not fully understand the detailed etiology and pathology of this injury. Finite element (FE) modeling is well suited for studying the mechanical response of the head and brain to blast loading. This paper details the development of a FE head and brain model for blast simulation by examining both the dilatational and deviatoric response of the brain as potential injury mechanisms. The levels of blast exposure simulated ranged from 50 to 1000 kPa peak incident overpressure and 1–8 ms in positive-phase duration, and were comparable to real-world blast events. The frontal portion of the brain had the highest pressures corresponding to the location of initial impact, and peak pressure attenuated by 40–60% as the wave propagated from the frontal to the occipital lobe. Predicted brain pressures were primarily dependent on the peak overpressure of the impinging blast wave, and the highest predicted brain pressures were 30% less than the reflected pressure at the surface of blast impact. Predicted shear strain was highest at the interface between the brain and the CSF. Strain magnitude was largely dependent on the impulse of the blast, and primarily caused by the radial coupling between the brain and deforming skull.The largest predicted strains were generally less than 10%, and occurred after the shock wave passed through the head. For blasts with high impulses, CSF cavitation had a large role in increasing strain levels in the cerebral cortex and periventricular tissues by decoupling the brain from the skull. Relating the results of this study with recent experimental blast testing suggest that a rate-dependent strain-based tissue injury mechanism
is the source primary blast TBI.

REPORT DOCUMENTATION PAGE (SF298)
(Continuation Sheet)

Continuation for Block 13

ARO Report Number 58155.14-LS-MUR
Development of a Finite Element Model for Blas ...

Block 13: Supplementary Note
© 2012 . Published in Annals of Biomedical Engineering, Vol. Ed. 0 (2012), (Ed.). DoD Components reserve a royalty-free, nonexclusive and irrevocable right to reproduce, publish, or otherwise use the work for Federal purposes, and to authroize others to do so (DODGARS §32.36). The views, opinions and/or findings contained in this report are those of the author(s) and should not be construed as an official Department of the Army position, policy or decision, unless so designated by other documentation.

Approved for public release; distribution is unlimited.

Annals of Biomedical Engineering (© 2012)
DOI: 10.1007/s10439-012-0519-2

BMES BIOMEDICAL ENGINEERING SOCIETY™ www.bmes.org

Development of a Finite Element Model for Blast Brain Injury and the Effects of CSF Cavitation

MATTHEW B. PANZER,[1] BARRY S. MYERS,[1] BRUCE P. CAPEHART,[2,3] and CAMERON R. BASS[1]

[1]Department of Biomedical Engineering, Duke University, 136 Hudson Hall, Box 90281, Durham, NC 27708, USA; [2]OEF/OIF Veterans Program and Mental Health Service Line, Durham VA Medical Center, 508 Fulton St., Durham, NC 27705, USA; and [3]Department of Psychiatry and Behavioral Sciences, Duke University School of Medicine, Durham, NC, USA

(Received 21 September 2011; accepted 19 January 2012)

Associate Editor Stefan M. Duma oversaw the review of this article.

Abstract—Blast-related traumatic brain injury is the most prevalent injury for combat personnel seen in the current conflicts in Iraq and Afghanistan, yet as a research community, we still do not fully understand the detailed etiology and pathology of this injury. Finite element (FE) modeling is well suited for studying the mechanical response of the head and brain to blast loading. This paper details the development of a FE head and brain model for blast simulation by examining both the dilatational and deviatoric response of the brain as potential injury mechanisms. The levels of blast exposure simulated ranged from 50 to 1000 kPa peak incident overpressure and 1–8 ms in positive-phase duration, and were comparable to real-world blast events. The frontal portion of the brain had the highest pressures corresponding to the location of initial impact, and peak pressure attenuated by 40–60% as the wave propagated from the frontal to the occipital lobe. Predicted brain pressures were primarily dependent on the peak overpressure of the impinging blast wave, and the highest predicted brain pressures were 30% less than the reflected pressure at the surface of blast impact. Predicted shear strain was highest at the interface between the brain and the CSF. Strain magnitude was largely dependent on the impulse of the blast, and primarily caused by the radial coupling between the brain and deforming skull. The largest predicted strains were generally less than 10%, and occurred after the shock wave passed through the head. For blasts with high impulses, CSF cavitation had a large role in increasing strain levels in the cerebral cortex and periventricular tissues by decoupling the brain from the skull. Relating the results of this study with recent experimental blast testing suggest that a rate-dependent strain-based tissue injury mechanism is the source primary blast TBI.

Keywords—Finite element model, Blast overpressure, Blast injury, Traumatic brain injury, Injury mechanism, CSF cavitation.

Address correspondence to Matthew B. Panzer, Department of Biomedical Engineering, Duke University, 136 Hudson Hall, Box 90281, Durham, NC 27708, USA. Electronic mail: matthew.panzer@duke.edu, barry.myers@duke.edu, bruce.capehart@va.gov, dale.bass@duke.edu

INTRODUCTION

Since 2004, U.S. military hospitals and Veterans Administration (VA) medical centers have seen convincing evidence of an increase in traumatic brain injuries (TBI) in military personnel, largely attributed to blast-related events.[38,53] Improvised explosive devices (IEDs) were the source of nearly 80% of the casualties reported to the Joint Theater Trauma Registry (JTTR) from 2001 to 2005.[39] The use of hard-plated thoracic armors increases the human threshold to blast exposure, causing a shift in vulnerability from the thorax to the head.[56] Early reports estimated the incidence rate of TBI in combat veteran is between 13 and 22%.[49,51] Blast-related TBI have both acute and chronic sequellae, and detailed etiology and pathology are still not fully understood.[10]

Blast-related neurotrauma research has focused on primary blast injuries, produced by the direct impingement of the pressure wave on the head rather than from fragment penetration (secondary), blunt impact (tertiary), or chemical/thermal (quaternary) exposure.[4] Finite element (FE) modeling is well suited for studying the mechanical response of the head to primary blast loading, and researchers have recently developed FE models to improve our understanding of blast TBI (Table 1).[9,11,30,32,37,40,50] However, current FE models for brain injury are exploratory until a robust set of validation data is available.

A major limitation of some current blast models is that their loading conditions are not representative of real-world blast events. Typical IED exposures resulting in blast injury were reported to be from detonations of 105- and 155-mm artillery rounds (equivalent to 2.4 and 7.3 kg TNT, respectively) at a standoff distances between 5 and 10 m.[33] The Conventional Weapons Effects Program

© 2012 Biomedical Engineering Society

Published online: 02 February 2012

TABLE 1. A survey of FE models for blast brain injury and their blast loading conditions (CONWEP calculations in parenthesis).

Study	Head model type and mesh details	Charge size (kg TNT)	Standoff (m)	Peak incident overpressure (kPa)	Duration (ms)
Cronin *et al.*[11]	Plane Strain Model	(1.648)	(1.65)	427	2.0
	No details given	(5.775)	(2.84)	330	3.0
		(24.3)	(5.21)	247	5.0
Moore *et al.*[30]	3D model	0.0648	0.60	506 (377[b])	(0.67)
Nyein *et al.*[37]	808,766 tet elements	0.324	0.60	1834 (1259[b])	(1.11)
	2.9 mm (mean size)[a]	0.00316	0.12	(1452)	(0.21)
Moss *et al.*[32]	3D model	2.944[c]	4.60	(1001[d])	(4.28[d])
	No mesh details given				
Taylor and Ford[50]	3D model	3.18[b]	2–3 (1.266[b])	1300	(2.35)
	1 mm (voxel)				
	Hexahedral				
Chafi *et al.*[9]	3D model	0.038	0.80	(133)	(0.76)
	27,971 hex elements	0.093	0.80	(258)	(0.78)
	5.2 mm (mean size)[a]	0.227	0.80	(507)	(1.06)
Panzer *et al.*[40]	Plane strain model	(0.291)	(2.55)	50	2.0
	7650 hex elements	(0.501)	(2.16)	100	2.0
	1.5 mm (mean size)	(1.31)	(2.16)	200	2.0
		(1.56)	(1.53)	500	2.0
		(1.42)	(1.09)	1000	2.0
		(13.5)	(1.67)	2000	2.0
		(7.85)	(7.65)	50	6.0
		(13.5)	(6.47)	100	6.0
		(35.4)	(6.49)	200	6.0
		(41.8)	(4.58)	500	6.0
		(39.0)	(3.29)	1000	6.0

[a]Estimated from a head volume of 4000 cm^3 (*Note*: It takes five tet elements to make one hex element).
[b]Discrepancy between reported value and CONWEP calculation.
[c]Equivalent charge size in TNT.
[d]Based on hemispherical blast CONWEP calculations.

(CONWEP)[20] can calculate the blast exposures produced from these charges, and indicate that the real-world blast threat ranges from 50 to 1000 kPa peak overpressure and 2–6 ms in duration. Many FE models simulate exposures based on small charge sizes (<1 kg TNT) at a very close standoff (<1 m),[9,30,37] which may reproduce realistic peak overpressure but very low positive-phase duration or impulse.[20] Additionally, models that do simulate real-world blast events only consider a single blast condition,[32,50] making it difficult to assess the biomechanics that may cause injury from blast impact. Pulmonary blast injury risk is dependent on both peak overpressure and duration (or impulse), and it is hypothesized that the injury mechanisms associated with short duration blasts differ from those associated with long duration blasts (cf. Panzer *et al.*[42]). Furthermore, recent experimental research using animal models suggested that blast TBI may also be dependent on peak overpressure and duration,[44,45] implying that computational models need to simulate a wide range of blast exposures to understand the potential injury mechanisms.

An additional question in FE blast modeling is how CSF cavitation formation and collapse affects the mechanical response of the brain to blast loading. CSF cavitation has long been speculated to be a brain injury mechanism for blunt impacts[24,36] and blast,[31] but only a few FE blast brain studies have included CSF cavitation in the model.[32,40,54]

This paper details the development of a FE head and brain model for simulation of exposures comparable to real-world blast events. The model provides insight into the biomechanics of primary blast exposure to the head by examining the dilatational and deviatoric response of the brain as potential mechanisms for blast brain injury. This study also investigates the response of the brain to the presence of CSF cavitation. The results of this study can guide blast modeling and experimentation, and provides a foundation to investigate and design blast protective countermeasures.

MATERIALS AND METHODS

We developed a plane-strain FE model of the human head and brain and positioned it within a blast domain model using the LS-Dyna hydrocode (v971.R5.1; Livermore Software Technologies Corp., Livermore, CA), and ran all simulations for 10 ms with a time step of 82 ns.

Head Model

Model geometry was based on an axial slice photo of the high-resolution (0.33 mm/pixel, 0.33 mm slice thickness) female dataset (age: 59, height: 1.65 m) from the Visible Human Project[1] at the anterior-most portion of the frontal lobe (Fig. 1). The scalp was modified to remove the excess posterior skin, and the geometry was scaled to match the head anthropometry of the 50th percentile male US Army personnel.[15] The model consisted of seven parts: CSF (including ventricles), grey matter, white matter, deep nervous tissue (thalamus, caudate and lentiform nucleus), inner and outer tables, diploë, and scalp. A 2 mm thick CSF layer was added between the skull and cerebral cortex,[23] and the diploë was set to 40% of the skull thickness.[25]

Previous blast FE analysis showed the deviatoric response in a solid was highly sensitive to solid mesh sizes during blast simulation.[41] Coarser solid meshes under-predict stress magnitude compared to finer solid meshes with the same loading conditions, particularly in locations of stress concentration such as at the interface between the skull and the brain. To ensure that the model captured these local stress gradients, the head mesh size was selected based on the results of a mesh convergence study using the same blast conditions in this study (see Electronic Supplementary Material). The head mesh comprised of a single layer of 29,088 hexahedral Lagrangian elements (1 mm thick) with an average characteristic length of 0.8 mm, which is more refined than most other blast models (Table 1). Based on a mesh convergence study on this model the current head mesh had a 3% error in peak stress distribution in the brain compared to a head mesh twice as refined (Online Appendix A).

High rate material properties where emphasized when choosing materials for head model (Table 2). The deviatoric response of brain tissue was modeled using a linear viscoelastic (LVE) constitutive model based on experimental data of white matter tested in shear up to 6300 Hz.[34] Grey matter and the deeper nervous tissues materials were based on their relative stiffness to white matter: white matter was 50% stiffer than grey matter,[22] and the thalamus was 30% stiffer than white matter.[43] Since the regional variation of brain tissue relaxation was not significant,[43] the reduced relaxation function of each brain material remained the same. The deviatoric response of skull and scalp materials were also modeled using LVE constitutive models,[14,28,29] and the dynamic viscosity of CSF at body temperature was included in the CSF material model.[7]

The volumetric response of CSF, brain tissue, and scalp were modeled using the Mie-Gruneisen equation of state (EOS) (Eq. (1)) using the constants for water.[26] The volumetric response of the skull was based on linear elasticity (i.e. constant speed of sound). While the linear elastic EOS describes the volumetric response similarly to the Mie-Gruneisen EOS for the low levels of volumetric compression seen in these simulations (<0.5%), it may be insufficient for describing pressure wave propagation through the material and at transmission interfaces for more severe blast cases with higher pressures.

$$P_{\mathrm{EOS}} = \rho_0 C^2 \mu \frac{1-(1-\gamma/2)\mu}{[1-(S_1-1)\mu]^2} \quad \text{for } \mu > 0 \text{ (compression)}$$
$$P_{\mathrm{EOS}} = \rho_0 C^2 \mu \quad \text{for } \mu < 0 \text{ (expansion)},$$
$$\text{where } \mu = \frac{\rho}{\rho_0} - 1 \tag{1}$$

Models with and without CSF cavitation were simulated since it remains unclear whether CSF cavitation occurs within the skull during a blast event. Cavitation was modeled using the cut-off pressure

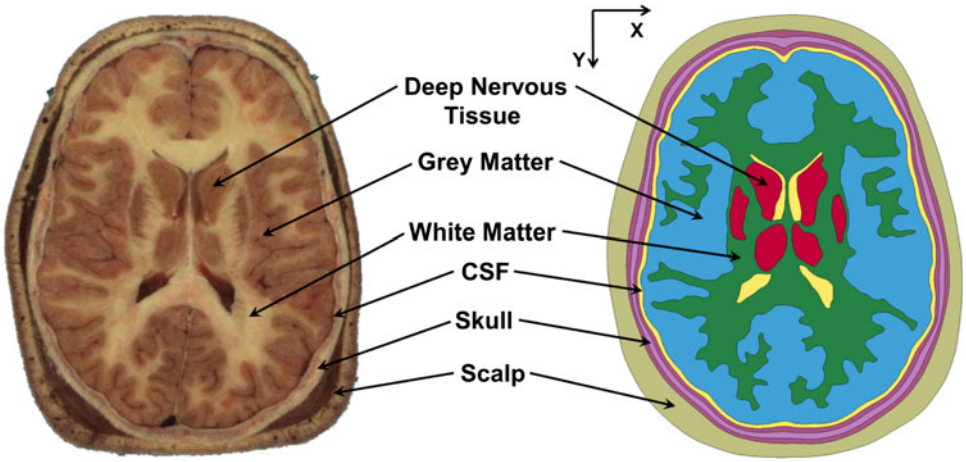

FIGURE 1. Brain geometry from photo (left; Visible Human Project) and plane-strain model (right).

TABLE 2. Summary of material properties in the model.

Part	Component	Material parameters		
		Bulk properties	Shear properties	
Brain	White matter	$\rho = 1.06$ g/cm^3	$G_1 = 50$ kPa	$\beta_1 = 100$ ms^{-1}
		$C = 1437$ m/s	$G_2 = 6.215$ kPa	$\beta_2 = 4.35$ ms^{-1}
		$S_1 = 1.979$	$G_3 = 2.496$ kPa	$\beta_3 = 0.2$ ms^{-1}
		$\Gamma_0 = 0.110$	$G_4 = 1.228$ kPa	$\beta_4 = 0.0053$ ms^{-1}
			$G_5 = 1.618$ kPa	$\beta_5 = 5.1e{-}6$ ms^{-1}
			$G_\infty = 0.27$ kPa	
Scalp		$\rho = 1.13$ g/cm^3	$G_1 = 355$ kPa	$\beta_1 = 0.005$ ms^{-1}
		$C = 1392$ m/s	$G_2 = 399$ kPa	$\beta_2 = 0.05$ ms^{-1}
		$S_1 = 1.979$	$G_3 = 35.6$ kPa	$\beta_3 = 0.5$ ms^{-1}
		$\Gamma_0 = 0.110$	$G_\infty = 408$ kPa	
CSF		$\rho = 1.00$ g/cm^3	$\mu = 0.8 \times 10^{-3}$ Pa s	
		$C = 1484$ m/s		
		$S_1 = 1.979$		
		$\Gamma_0 = 0.110$		
		$P_{cav} = -100$ kPa		
Skull	Inner & outer tables	$\rho = 2.00$ g/cm^3	$G_1 = 2289.6$ MPa	$\beta_1 = 0.03$ ms^{-1}
		$K = 10{,}227$ MPa	$G_2 = 4708.5$ MPa	$\beta_2 = 275$ ms^{-1}
			$G_\infty = 4720.3$ MPa	
	Diploë	$\rho = 1.30$ g/cm^3	$G_1 = 491.8$ MPa	$\beta_1 = 0.03$ ms^{-1}
		$K = 1297.4$ MPa	$G_2 = 1011.4$ MPa	$\beta_2 = 275$ ms^{-1}
			$G_\infty = 1013.9$ MPa	

method in LS-Dyna,[17] which limits the tensile pressure of the CSF passed a certain threshold (Eq. (2)). Cavitation pressure was set at −100 kPa, although this level can only been speculated.[24] Similar CSF cavitation methods and pressure thresholds were used in other head FE models.[32,40,54]

$$P = \max(P_{EOS}, P_{CAV}) \quad \text{for CSF cavitation} \qquad (2)$$

Blast Model

Previous blast FE analysis showed the volumetric response in a solid was highly sensitive to air mesh sizes during blast simulation.[41] Coarser air meshes underpredict pressure magnitude compared to finer air meshes with the same blast conditions, particularly in fast-rising pressure waves like at the shock front. In a blast simulation, the air mesh is often the largest computational cost in the model, and compromises are made between pressure wave accuracy and computational efficiency. The air mesh size was selected based on the results of a mesh convergence study using the same blast conditions in this study (see Electronic Supplementary Material). The blast was modeled using a single layer 308,000 hexahedral Eulerian mesh with a minimum length of 2 mm. Based on a mesh sensitivity analysis, the current air mesh had a 6% error in peak pressure distribution in the brain compared to an air mesh twice as refined, but only 25% the computational cost.

Compressible gas dynamics were calculated using a 2nd order van Leer advection scheme with half-shift-index[17]; Shocks were treated using an artificial bulk viscosity approach to eliminate oscillations from discontinuities by smearing the shock over three to five elements. In this study, the artificial bulk viscosity parameters were not modified from the default LS-Dyna parameters because this setting produced good shock fronts for the mesh size and overpressures simulated.[41] Furthermore, the pressure response of the brain model showed little sensitivity (±2%) to large variations of the bulk viscosity parameters (±100%), no sensitivity for the strain response, and spurious oscillations were minimal (Online Appendix B). Using these modeling conditions, this solver and setup reproduced the analytical solution for 1D shock tube response with good accuracy.[41] The fluid–structure interaction algorithm within LS-Dyna coupled the Lagrangian and Eulerian models.

The blast domain consisted of air modeled using the ideal gas law ($\gamma = 1.4$) with initial standard atmospheric conditions ($P_0 = 101$ kPa, $\rho_0 = 1.23$ g/mm^3). An optimization study aimed at reducing the size of the domain without introducing errors associated with the boundaries help determine the size the blast domain. The head was positioned in the middle of the blast domain with the front of the head model located 300 mm from the source boundary (Fig. 2).

The blast wave entered the model by prescribing thermodynamic state (pressure and density) and flow velocity at one boundary of the blast domain (Fig. 3).

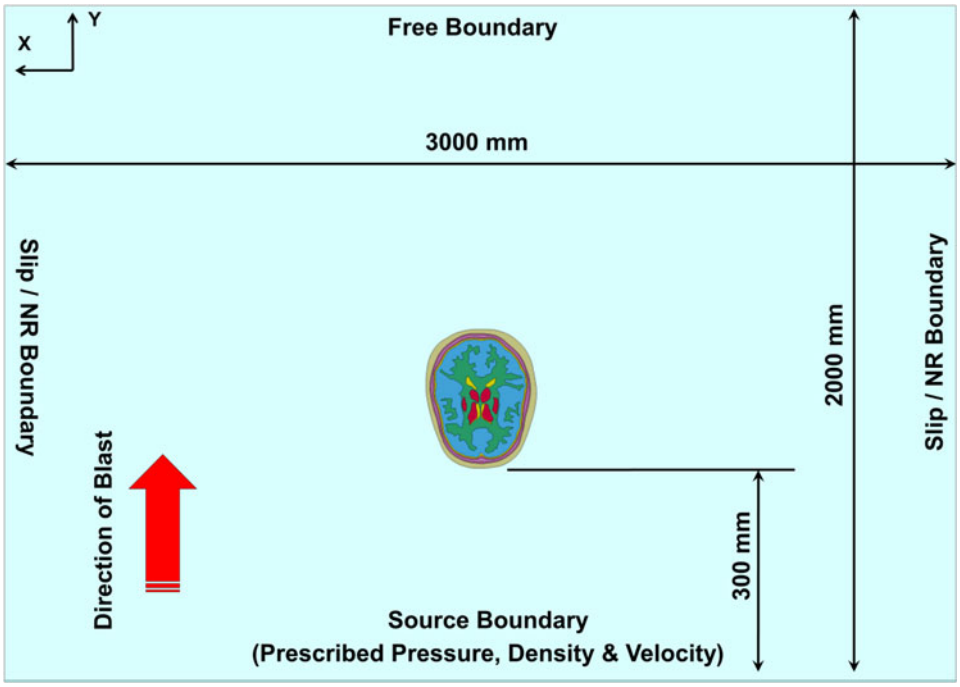

FIGURE 2. Layout of the blast domain (width and depth not to scale).

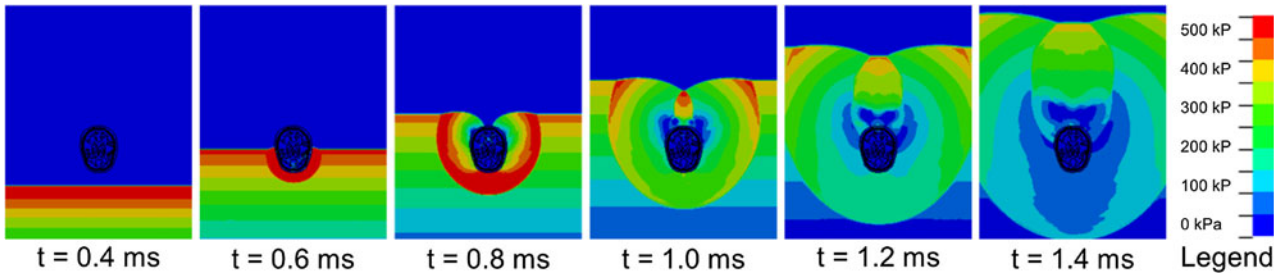

FIGURE 3. The time progression of pressure showing the impingement of the simulated blast wave on the head model (pressure in head not shown).

This technique allowed for a fully developed blast wave using a truncated domain (reducing the number of elements for computation). Initially, the sides of the domain were slip boundaries to maintain the planar nature of the blast wave. The boundary conditions were switched to non-reflecting boundaries (impedance-matched outflow to reduce the effects of the boundary) just prior to the reflected shock wave reaching the edges. This method of switching boundary types was crucial in reducing the total width of the blast domain while maintaining planar blast wave conditions for most of the simulation (Fig. 3, Video—Electronic Supplementary Material). The boundary opposite the source was modeled as a free boundary (Dirichlet boundary with ambient pressure conditions), which was more representative of the infinite-domain response than using a non-reflecting boundary treatment because the flow conditions were advection-dominant (verified using a much larger domain size).

Blast Conditions

We simulated eighteen different cases with blast waves ranging between 50 and 1000 kPa peak incident overpressure, and between 1 and 8 ms of positive phase duration (Fig. 4). These cases range over a number of previously defined blast injury criteria,[5,45,46] and span a range of pressures and durations commonly seen during combat operations. The peak overpressure-duration characteristics for two commonly used munition types (for standoffs between 1 and 15 m) were calculated using CONWEP and included as a real-world reference to the blast conditions simulated.

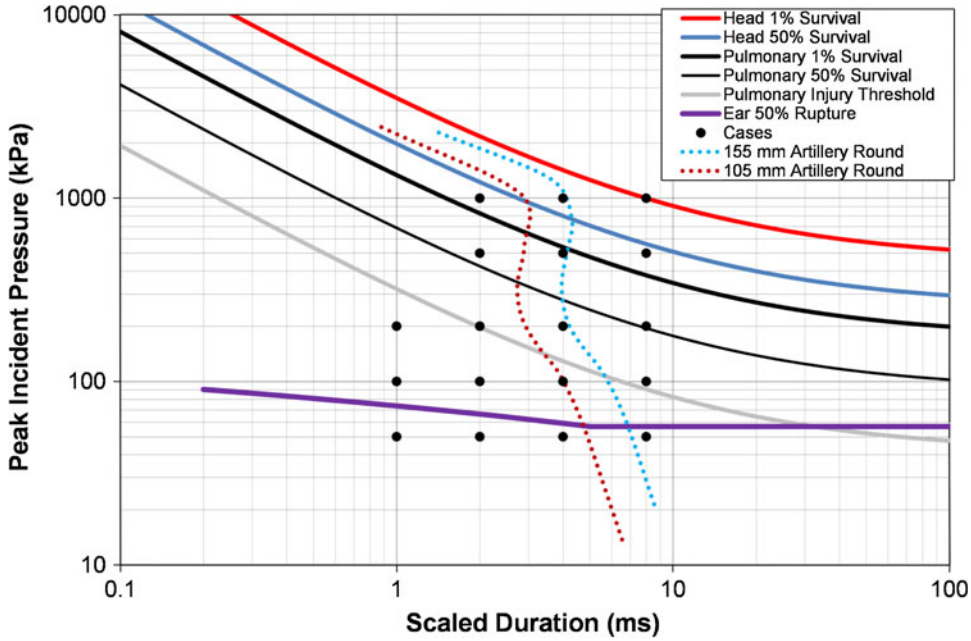

FIGURE 4. Peak incident overpressure and duration conditions for blast simulation compared to human primary blast injury criteria and real-world blast threats.

Statistical Methods

A univariate general linear model was used to assess the effect of the blast wave parameters (peak overpressure, duration, impulse) on the mechanical response of the brain, using the 95th percentile peak value response (pressure, von Mises stress, maximum shear strain, strain rate) as the outcome. Peak incident overpressure and incident impulse were converted to peak reflected overpressure and reflected impulse using the Rankine-Huigoniot relations,[21] because the reflected pressure is more representative of the loaded applied to the head than the free-stream incident pressure. Test for significance was 5% ($\alpha = 0.05$).

RESULTS

A summary of the results for the non-cavitating and cavitating head models exposed to eighteen blast conditions of varying severity is shown in Table 3. To avoid having the values from a single element characterize the response of the brain, the pressure, stress, strain and strain rates listed in Table 3 are the 95th percentile peak values from that particular blast condition. Coefficients for the general linear model are shown in Table 4.

Dilatational Response to Blast

Regardless of severity, the largest pressures measured throughout most of the brain were from the initial brain shock wave produced from the blast wave impacting the head. The highest values of peak brain pressure were concentrated in the frontal portion of the brain corresponding to blast impact site on the head (Fig. 5), and attenuated 40–60% as the wave propagated from the frontal lobe to the occipital lobe. Peak pressures in the brain were 30% less than the peak reflected pressure measured at the surface of the head.

CSF cavitation produced a number of localized high-pressure regions in brain tissues adjacent to the CSF, including the periventricular tissues, caused by cavitation collapse (Fig. 5). This phenomenon appeared in the most severe blast conditions (conditions 8–18), but only in the largest impulse blast cases (conditions 15 and 18) did the effects of CSF cavitation contribute to an increase in peak brain pressure greater than 4% over the non-cavitating model (Table 3).

For the non-cavitating model, peak brain pressure was only dependent on the peak pressure of the blast wave ($p < 0.001$), and not the blast duration ($p = 0.93$) or blast impulse ($p = 0.16$). In the cavitating head model, peak brain pressure was dependent on the peak pressure and impulse of the blast wave ($p < 0.001$ and $p = 0.007$, respectively), while blast duration was not significant ($p = 0.31$). Impulse was a significant factor for the pressure distribution in the cavitating model because increasing impulse exacerbated the amount of cavitation for a given blast peak overpressure condition, leading to more cavitation collapses and localized high-pressure regions.

TABLE 3. Summary of the peak brain tissue responses (95th percentile) for each blast condition.

Blast conditions					Non-cavitating model				Cavitating model			
Incident overpressure (kPa)	Duration (ms)	Incident impulse (kPa ms)	Charge size (kg TNT)	Charge distance (m)	Pressure (kPa)	von Mises stress (Pa)	Shear strain (%)	Strain rate (s^{-1})	Pressure (kPa)	von Mises stress (Pa)	Shear strain (%)	Strain rate (s^{-1})
50	1	17.1	0.037	1.28	65.7	19.5	0.07	12.3	65.7	19.5	0.08	12.3
50	2	34.1	0.291	2.55	68.9	30.2	0.14	13.0	68.9	30.2	0.14	13.0
50	4	68.3	2.33	2.10	70.6	36.4	0.20	13.0	70.6	36.4	0.20	13.0
50	8	136.6	18.6	10.2	71.5	52.7	0.30	13.6	71.5	52.7	0.30	13.6
100	1	27.9	0.063	1.08	161.9	36.8	0.16	14.3	161.7	36.7	0.16	14.2
100	2	55.7	0.501	2.16	163.2	62.3	0.32	15.7	163.2	62.3	0.32	15.7
100	4	111.4	4.01	4.32	166.2	92.8	0.51	17.1	166.2	92.7	0.51	17.1
100	8	222.4	31.9	8.62	168.4	138.9	0.75	21.6	170.5	138	0.72	25.4
200	1	51.4	0.168	1.09	398.2	86.8	0.44	21.0	398.4	86.5	0.44	30.4
200	2	101.8	1.31	2.16	414.6	119.0	0.58	23.9	415	124.2	0.58	39.3
200	4	204.1	10.5	4.33	422.0	178.3	0.91	29.7	423.3	186.6	0.93	54.9
200	8	407.7	83.9	8.65	407.7	236.6	1.26	35.2	421.6	232.3	1.20	68.6
500	2	157.9	1.56	1.53	1414.3	324.9	1.28	62.2	1416.5	301.3	1.40	128.3
500	4	314.7	12.4	3.05	1461.8	453.3	2.08	75.8	1466	490.2	2.43	172.6
500	8	629.5	98.8	6.10	1495.3	688.0	3.88	87.2	1716.1	892.5	4.75	221.6
1000	2	200.6	1.42	1.09	3680.3	671.0	2.83	134.5	3681.8	811	3.65	317.4
1000	4	403.0	11.5	2.19	3810.1	1233.1	6.04	175.1	3931.1	1701.5	8.48	547.0
1000	8	806.1	92.0	4.38	3900.7	1742.5	8.72	222.4	5805.1	4593.9	21.84	960.5

Overpressure durations within the brain caused by the initial impact of the shock wave ranged from 0.3 to 1.2 ms, substantially less than the overpressure duration of the incident blast waves (1–8 ms) (Fig. 6a). Following the initial shock wave, the non-cavitating model had transient brain pressures dominated by frequencies at 305, 610, and 6300 Hz regardless of blast level (Fig. 6b). In the cavitating model, the presence of CSF cavitation limited the amount of tensile pressure experienced in the brain tissue, and effectively dampened out much of the post-blast transient pressure response (Fig. 6a). Cavitation occurred early in the simulation, and was not associated with the negative pressure-phase of the blast.

Deviatoric Response to Blast

The highest shear strains and von Mises stresses were concentrated in the cerebral cortex at the interface between the brain and the CSF (Fig. 7). High von Mises shear stresses were also located deeper in the brain at grey-white matter interfaces. Deformation of the deeper tissues was typically 4–6 times less than in the cerebral cortex. The peak strain levels measured in both the cavitating and non-cavitating models were all less than 10% strain except for the largest blast case using the cavitating CSF model. The highest tissue strains developed later in the simulation after the initial blast wave had passed through the head (Fig. 8a). Long-term brain deformation was caused by the Radial coupling mechanics between the brain and the skull, which was oscillating in a flexural mode excited by the blast impact.

CSF cavitation had a greater effect on the deformation of the brain than it did on the pressure response (Fig. 7). The presence of cavitation caused the brain tissue to decouple from the skull, allowing the less-constrained brain material to deform more easily. The largest relative increases in brain tissue strain caused by CSF cavitation were in the occipital region of the brain, and in the periventricular tissues (Fig. 8b). There was less than 5% difference in peak stress/strain between the cavitating and non-cavitating model for the blast conditions with less than 200 kPa peak incident pressure (Table 3). However, for blast conditions 15–18 the cavitating model had more than a 20% increase in the peak stress/strain than the non-cavitating model.

For the non-cavitating model, the peak brain shear strain was dependent on the both the peak pressure and impulse of the blast wave ($p < 0.001$ for both respectively), and not the blast duration ($p = 0.43$). In the cavitating model, only the blast impulse was a contributing factor for the shear strain in the brain ($p = 0.003$), while blast peak pressure and duration was not significant ($p = 0.11$ and $p = 0.32$, respectively). Analysis on the stress response of the brain showed the same findings.

Strain rates were greater in the cavitating model than the non-cavitating model (Table 3). Peak strain rates coincided with CSF cavitation collapse, and the highest peak strain rates were in the cerebral cortex and the periventricular tissues. Strain rate was dependent on peak pressure and impulse for both models, but not duration.

TABLE 4. Coefficients for the general linear model of the peak brain tissue responses (95th percentile) to the blast conditions.

	Non-cavitating CSF model					Cavitating CSF model				
Brain outcome	R^2	Peak ref. pressure (kPa)	Duration (ms)	Ref. impulse (kPa ms)	β_0	R^2	Peak ref. pressure (kPa)	Duration (ms)	Ref. impulse (kPa ms)	β_0
Pressure (kPa)	0.999	**0.681 (0.009)**	−0.623 (6.68)	0.031 (0.021)	−44. 8 (24.8)	0.970	**0.622 (0.060)**	−47.33 (44.80)	**0.441 (0.140)**	−67.06 (166.6)
VM stress (Pa)	0.958	**0.137 (0.020)**	−12.1 (15.1)	**0.226 (0.047)**	−16.1 (56.0)	0.823	0.159 (0.095)	−73.37 (71.61)	**0.767 (0.223)**	−79.55 (266.3)
Shear strain (%)	0.953	**5.77×10^{-4} (1.02×10^{-4})**	−0.064 (0.079)	**1.31×10^{-3} (2.40×10^{-4})**	−0.088 (0.293)	0.836	7.39×10^{-4} (4.41×10^{-4})	−0.343 (0.330)	**3.73×10^{-3} (1.02×10^{-3})**	−0.379 (1.23)
Strain-rate (s^{-1})	0.982	**0.024 (0.002)**	−1.00 (1.30)	**0.018 (0.004)**	6.06 (4.82)	0.900	**0.067 (0.016)**	−11.5 (12.1)	**0.124 (0.038)**	−17.9 (45.0)

Parameter estimate in general linear model (standard error).
Bold denotes significance ($p < 0.05$).

Skull Response to Blast

The radial coupling between the brain and the skull was a major source of both the pressure and stress response throughout the brain following the initial exposure to the blast wave. Upon impact of the blast, the skull in the non-cavitating model would oscillate at a frequency of approximately 305 Hz in the first flexural mode, where the strain of the head length was out of phase with the strain of the head breadth (Fig. 9a). This mode shape and frequency was consistent for all blast conditions, with only the magnitude of the deformation varying with blast condition. In the cavitating CSF model, skull deformation amplitude was much larger than in the non-cavitating model but the mode shape remained the same (Fig. 9a). Decoupling the brain from the skull due to CSF cavitation also caused the skull to oscillate at a lower frequency than in the non-cavitating model (Fig. 9b).

DISCUSSION

We developed a detailed model of the human head for the simulation of the brains response to a wide range of real-world threats. Since a robust set of experimental data was not currently available for validating any human head model in blast, it was more practical to develop an exploratory plane-strain blast model before attempting to develop a complex 3D head model. We can examine many of the important aspects of numerical blast modeling in detail using this model, where it is often not feasible on a more complicated model.

One such advantage was that the mesh could be spatially resolved to capture the high-frequency waves associated with blast: the shock wave from a free-field blast has relevant frequency content up to 40 kHz.[3] When wave propagation is considered important in an FE model, the mesh should be six to ten elements per wavelength in order to reduce numerical dispersion.[6] At ten elements per wavelength, the current air and head mesh sizes could effectively propagate pressure waves with frequencies up to 18 kHz in air, and 140 kHz in brain tissue without accumulating significant numerical dispersion. However, with brain tissue having a frequency-dependent shear speed ranging from 1 to 1.5 m/s,[48] the model may only be effective in propagating pure shear waves for frequencies up to 150 Hz. Further mesh refinement to capture shear wave frequencies up to the skull resonant frequencies may be required, and should be confirmed with further mesh convergence studies. Another consideration for using a fine FE mesh is that proper use of artificial bulk viscosity will smear the shock over three to five

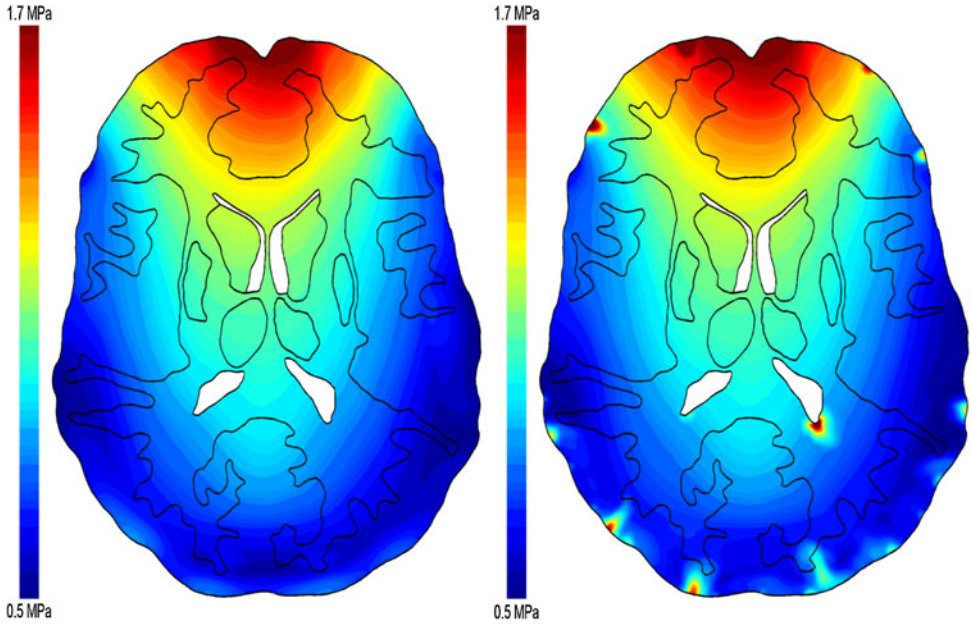

FIGURE 5. Comparison of the distributions peak brain tissue pressure between the non-cavitating (left) and cavitating (right) models for the 500 kPa/4 ms blast condition.

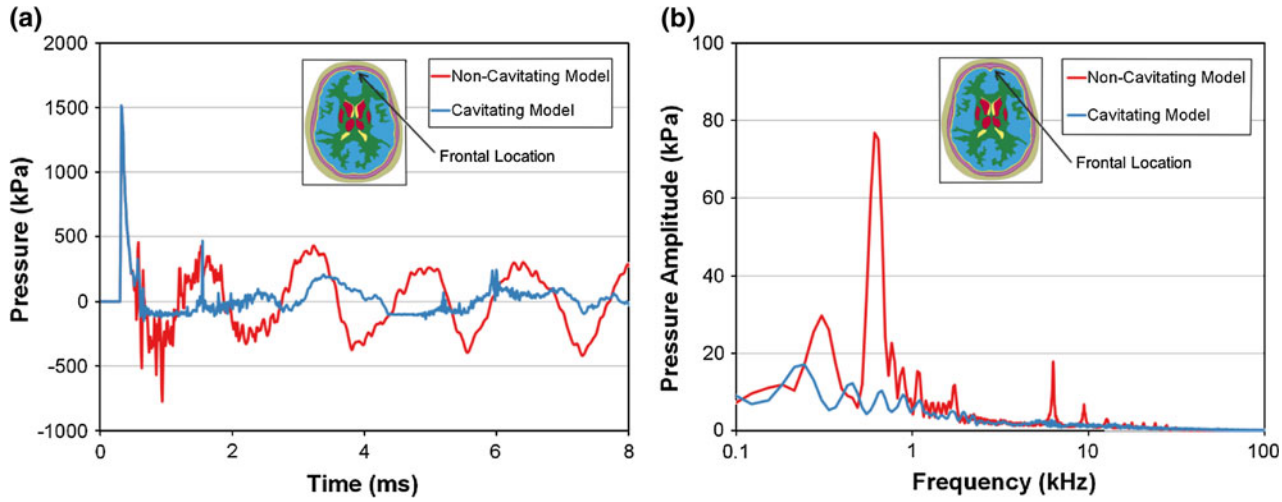

FIGURE 6. (a) Comparing the time-history and (b) frequency spectrum for the pressure in the frontal portion of the brain between the models for the 500 kPa/4 ms blast condition.

elements,[55] resulting in longer pressure rise times for coarser meshes or incorrect bulk viscosity settings.

However, there were limitations to using a plane-strain approach. In a 3D environment, the aerodynamics of the head allow for the blast to better flow around the head, so in this sense the plane-strain model was conservative. The model does not consider out-of-plane motion of the head, which might be important for brain shear stain if sagittal rotation develops following exposure. Anatomical features not represented in the model (face, orbits, paranasal sinuses, etc.) may influence the transmission of the shock wave into the brain during a frontal blast. The variation of the skull properties (thickness and microstructure) through the sagittal and coronal planes potentially introduces a different frequency response in the skull than those modeled with the plane-strain approach.

We recognize these limitations, and consider that the magnitudes of the biomechanical measures (pressure, strain) and the frequency spectrum of these transients predicted with the plane-strain model will likely change in the 3D environment. Ruan *et al.*[47] compared the strain and pressure response of a

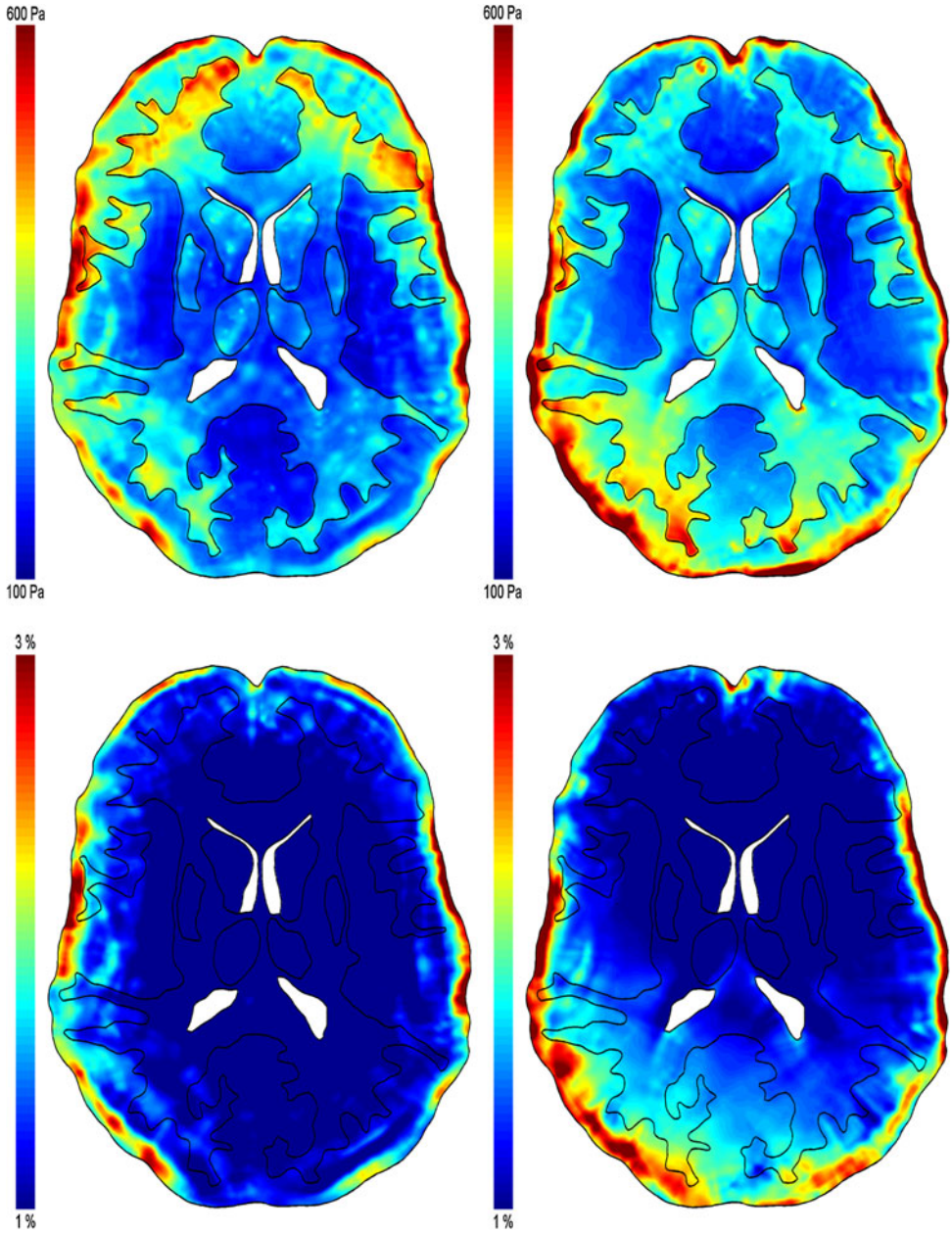

FIGURE 7. Comparison of the distributions of peak von Mises stress (top) and shear strain (bottom) between the non-cavitating (left) and cavitating (right) models for the 500 kPa/4 ms blast condition.

plane-strain model of the head (coronal slice) with an axisymmetric model of similar size, subjected to an impact loading. They found that the axisymmetric model was much stiffer than the plane-strain model, which resulted in strains in the plane-strain model up to 12 times larger than in the axisymmetric model.[47] To confirm these results, we compared the response of an axisymmetric spherical model to blast loading[41] to the response in a plane-strain spherical model with the same radial dimensions, material properties, and loading conditions. The plane-strain model had peak shear strains approximately seven times larger than the axisymmetric model, and peak pressures approximately 1.5 times larger, making the plane-strain assumption conservative for blast brain injury modeling. The increase in strain was from the greater compliance and loading of the plane-strain model, and the increase in pressures was from less attenuation of the pressure wave from being constrained in plane. Thus, the conclusions in this study were based on the relative effects of the brains response to certain parameters (either blast conditions or cavitation), providing insight into the response of skull and brain to blast exposure.

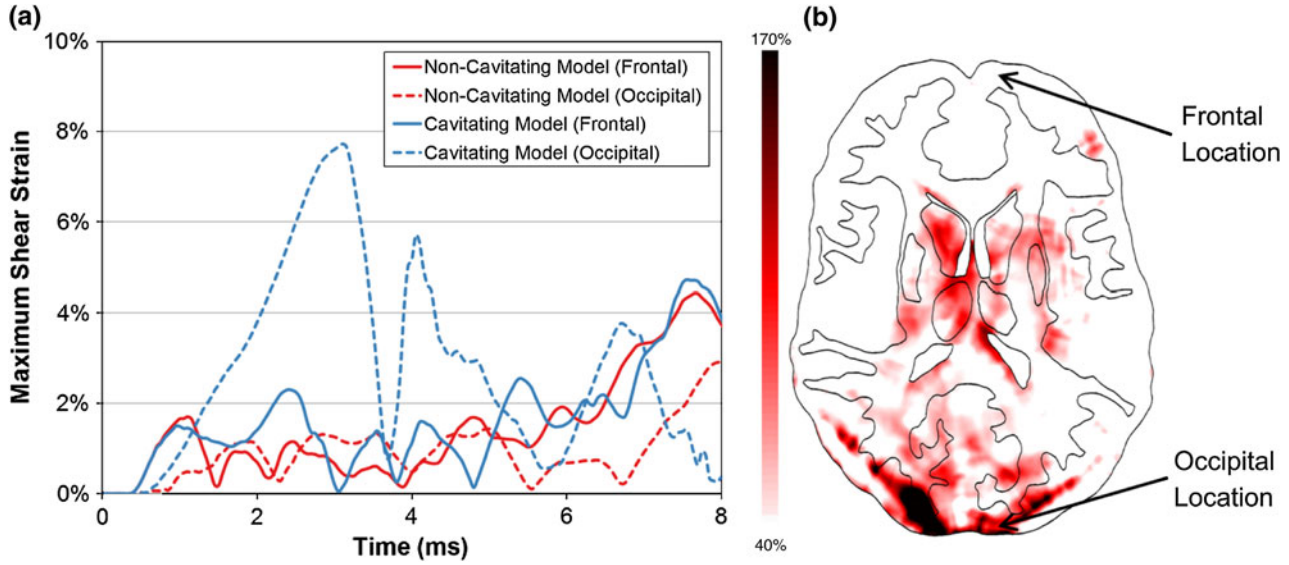

FIGURE 8. (a) Comparing the time-history for shear strain in the frontal and occipital portions of the brain between models and (b) the distribution of the relative increase in the peak brain strain due to cavitation for the 1000 kPa/4 ms blast condition.

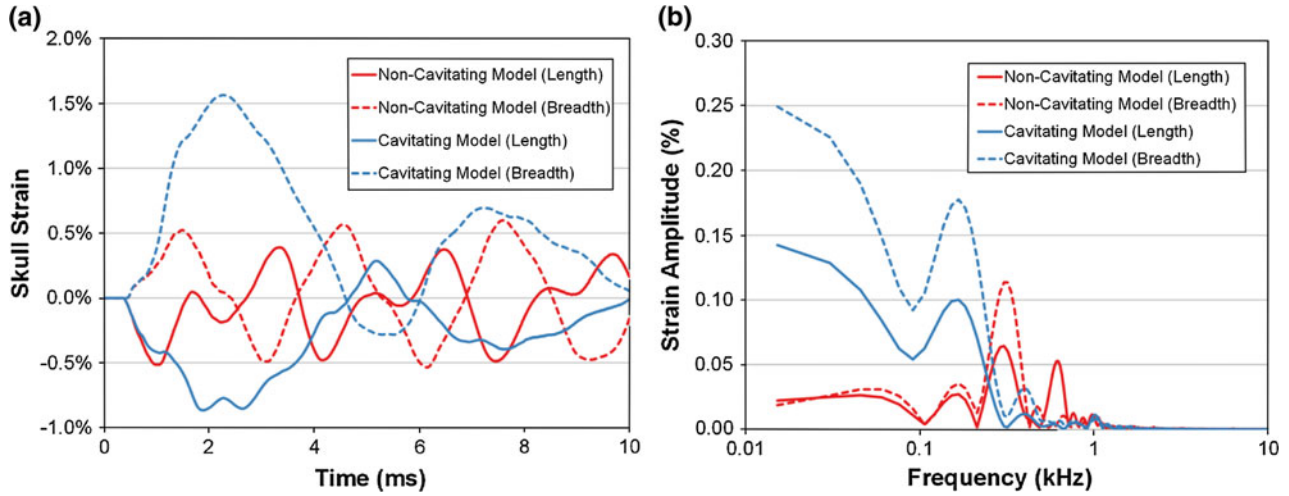

FIGURE 9. (a) Comparing the time-history and (b) frequency spectrum of the skull strain between the models for the 500 kPa/4 ms blast condition.

Brain Response to Blast

Over the wide range of blast conditions simulated, the maximum pressure levels within the brain were primarily dependent on the overpressure conditions of the blast wave. The insensitivity of pressure response to the blast duration was likely because the speed of sound in the skull and brain were much quicker than that of air. The higher sound speed propagated pressure away from the impact site faster than it was loaded, as evidenced by the 0.8–1.2 ms pressure pulse in the brain compared to the 1.0–8.0 ms pressure pulse of the blast. The length of the overpressure pulse in the brain tissue is likely an important consideration for *ex vivo* tissue studies attempting to replicate the internal conditions of blast exposure.

The deviatoric response of the brain was driven largely by skull deformation and not head motion (i.e., rigid body inertia), confirming previous computational results.[32] Strain developed mainly in the cerebral cortex as it moved relative to the vibrating skull. Decreasing the radial coupling between the brain and the skull (*via* CSF cavitation) increased the lag between the brain and skull and augmented strain levels. It is important to consider that maximum stresses and strains occurred after the initial shock wave passed through the head. Many FE models did not run

the simulation past 2 ms,[30,37,50] only capturing the response of the brain during the incident wave and not the response caused by the coupling between the brain and the deforming skull. If high-rate strain response from skull deformation following blast exposure is the primary mechanism for blast TBI, then it is critical that models are simulated long enough to capture these effects.

The skull deformation was primarily of the 1st mode of flexure, which had a natural frequency of approximately 305 Hz when the brain coupled with the skull and 169 Hz when CSF cavitation caused the brain to decouple. No evidence of localized skull flexure (skull ripple), as initially reported by Moss,[32] was seen in the simulations despite the plane-strain model being more susceptible to this type of deformation than an ellipsoid. The difference may be from modeling a skin layer over the skull. The skin likely attenuates pressure wave at the skull, and disperses the loading area so that the shock load is not concentrated locally on the skull. Regardless of these differences, it is apparent that skull deformation plays an integral role in the loading of the brain during blast exposure. Bolander *et al.*[8] recently demonstrated a correlation between skull strain and intracranial pressure in rats exposed to a shock wave, confirming the findings in this study. There is a need for empirical data on the deformation of human skulls exposed to blast loading to validate the skull mechanics in computational models.

Minimizing skull deformation may be an important consideration for improving helmet design in blast. The results of this study suggest that reducing the total impulse transferred to the head will reduce the amount of strain developed in the brain. Military helmet design strategies similar to those used for helmets that mitigate blunt impact forces (increased helmet-head standoff, energy-dissipative padding, etc.) are likely to reduce the skull deformation in blast. In a parametric study on helmet padding design for blast brain response, Panzer *et al.*[40] found that low-density crushable helmet padding best dissipated the energy transferred from the helmet to the head, and this resulted in lower brain strain.

Cavitation

CSF cavitation has long been hypothesized as a cause of brain injury in both automotive head impacts[24,36] and blast impacts.[31] However, it remains unclear whether CSF cavitation occurs during these impact events and at what tensile pressures. In laboratory conditions and devoid of nucleation sites, the cavitation pressure of water (by stretching) ranged from −100 kPa (aerated tap water) to −20 MPa (de-gassed distilled water).[18] Fluid cavitation pressure is dependent on a number of factors including temperature, surface tension, dissolved gas, presence of particles and nucleation sites.[18] Since the constituents of CSF differ from water, the pressure level at which CSF cavitation will occur may not be the same as water. Additionally, structures in the subarachnoid space may provide some tensile support that would alter the effective cavitation threshold of the CSF.

Few empirical studies exist on the cavitation phenomenon in CSF during inertial or impact loading to the skull, despite cavitation being an early hypothesis for the injury mechanism of concussion.[16] Impact studies using anthropomorphic surrogates have been able to reproduce cavitation in the brain and CSF,[24,35] but there is no direct empirical evidence that CSF cavitation occurs *in vivo* from in blast, blunt or inertial loading, not is there clinical evidence that cavitation is an injury mechanism.

The results of this study indicate that the presence of CSF cavitation at −100 kPa has a substantial impact on the response of the brain in more severe blast conditions. Wardlaw *et al.*[54] reported on the possibility for CSF cavitation to occur in blast using a 3D ellipsoid head model. In conclusions similar to this study, they found that the periodic formation of CSF cavitation and collapse was related to skull deformation. However, they did not quantify the effect of CSF on the mechanics of the brain. The current study found that in addition to creating localized regions of high pressure when the CSF cavitation collapsed (the mechanism for traditional cavitation damage), the presence of CSF cavitation allowed the brain to decouple from the skull resulting in an increase in brain strain. CSF cavitation also occurred early in the simulation because of the inertial and deformational effects between the brain and skull, and not during the negative pressure phase of the blast as previously hypothesized.[31]

CSF cavitation may also play a role in damaging deeper neural tissues. The periventricular tissues experienced higher levels of strain when CSF cavitation occurred in addition to the elevated levels of pressure from cavitation collapse. Periventricular white matter changes are commonly seen on MRI scans of persons with Alzheimer disease,[19] and diffuse radiation injury of the brain.[52] In this model, results show greater potential for tissue damage at anatomic locations that are with relatively poor blood supply compared to other brain regions.

Potential Injury Mechanisms

Despite the plane-strain model likely over-predicting the pressure levels in the brain, all pressures measured in the brain were much lower than the

hydrostatic threshold for cell death (approximately 100 MPa) measured in bacterial[27] and mammalian cells,[13] even in the most severe conditions simulated. This would indicate that either pressure is not an injury mechanism for brain tissue in blast, or that a pressure-based injury criterion will include rate effects that would decrease the tissue threshold from the hydrostatic criterion.

Maximum pressure levels within the brain were primarily dependent on the overpressure conditions of the blast wave, even in the presence of CSF cavitation, implying that if pressure was the only injury mechanism of brain tissue, then TBI should not depend on blast duration or impulse. This would be unlike short-duration pulmonary blast injury criteria where injury risk is strongly associated with both peak overpressure and duration.[42] Furthermore, recent experimental results using a thoracic-protected ferret model exposed to a wide range of blast conditions has shown strong exposure duration dependence for moderate/severe meningeal bleeding, apnea, and fatality.[44] By considering these animal tests along with the findings of this study, it would suggest that brain tissue pressure was not the sole injury mechanism for moderate to fatal brain injuries.

The model predicted brain tissue strain would increase with blast impulse, which agrees with the results found by Rafaels if the brain injury mechanism was strain-based. However, peak strain levels predicted in the tissue were typically much lower than strain levels thought to be associated with injury thresholds. Bain and Meaney[2] found electrophysiological impairment in axons of a guinea pig optic nerve model at a threshold of 18% strain. Elkin and Morrison reported a cortical cell death threshold between 10 and 20% strain in organotypic hippocampal slice cultures in addition to finding an increase of injury with strain rate.[12] Given the relatively low levels of strain for nearly all blast conditions simulated, a rate-dependent, strain-based injury mechanism is the likely source of brain injury.

An additional point to note is that this discussion on injury mechanism only considers moderate and severe TBI based on the work by Rafaels *et al.*[44] Currently, there are no published studies concerning mild TBI in any animal model with exposures over a wide range of peak overpressures and durations (or impulses). It is possible that the injury mechanisms responsible for gross injury of brain tissue in blast are not the same as mechanisms that are responsible for mild TBI. Furthermore, it has been previously shown that tissue injury thresholds can vary by region in the brain.[12] The increase in strain caused by CSF cavitation for periventricular tissues may exceed injury thresholds prior to tissue in the cortex, which has the largest predicted strains, but also the higher threshold for injury.

CONCLUSION

This paper reviews the development and simulation of a FE head and brain model for blast exposures. Unique to this approach is an emphasis on comparison to a wide range of real-world blast events by examining both the dilatational and deviatoric response of the brain as potential injury mechanisms. Peak pressures in the brain were primarily dependent on the peak overpressure of the impinging blast wave, while maximum brain strain was largely dependent on the impulse of the blast. Coupling between the brain and resulting skull deformations after the shock wave passed through the head induced the largest brain tissue strains. When considering the results from animal injury models, these computational finding suggest a rate-dependent strain-based injury mechanism as the source primary blast TBI. CSF cavitation had a large role in the response of the brain by increasing strain levels in the cerebral cortex and in the periventricular tissues. These findings may be important in how the biomechanics community approaches the study of neurotrauma mechanisms, and how we can relate the external parameters of blast to brain injury outcome.

ELECTRONIC SUPPLEMENTARY MATERIAL

The online version of this article (doi: 10.1007/s10439-012-0519-2) contains supplementary material, which is available to authorized users.

ACKNOWLEDGMENTS

This work funded in part by the Multidisciplinary Research Initiative (MURI) program (W911MF-10-1-0526; University of Pennsylvania as prime institution) through the Army Research Office (ARO). We also acknowledge the support of the James H. McElhaney Biomechanics Fellowship for one of the authors (M.B. Panzer).

REFERENCES

[1]Ackerman, M. J. The visible human project. *Proc. IEEE* 86:504–511, 1998.

[2]Bain, A. C., and D. F. Meaney. Tissue-level thresholds for axonal damage in an experimental model of central nervous system white matter injury. *J. Biomech. Eng.* 122:615, 2000.

[3]Bass, C. R., M. B. Davis, K. A. Rafaels, S. Rountree, *et al.* A methodology for assessing blast protection in explosive ordinance disposal bomb suits. *Int. J. Occup. Saf. Ergon.* 11:347–361, 2005.

[4]Bass, C. R., M. B. Panzer, K. A. Rafaels, G. W. Wood, *et al*. Brain injuries from blast. *Ann. Biomed. Eng*. 40:185–202, 2012.
[5]Bass, C. R., K. A. Rafaels, and R. S. Salzar. Pulmonary injury risk assessment for short-duration blasts. *J. Trauma* 65:604–615, 2008.
[6]Bazant, Z. P. Spurious reflection of elastic waves in non-uniform finite element grids. *Comput. Methods Appl. Mech. Eng*. 16:91–100, 1978.
[7]Bloomfield, I. G., I. H. Johnston, and L. E. Bilston. Effects of proteins, blood cells and glucose on the viscosity of cerebrospinal fluid. *Pediatr. Neurosurg*. 28:246–251, 1998.
[8]Bolander, R., B. Mathie, C. Bir, D. Ritzel, *et al*. Skull flexure as a contributing factor in the mechanism of injury in the rat when exposed to a shock wave. *Ann. Biomed. Eng*. 39:2550–2559, 2011.
[9]Chafi, M., G. Karami, and M. Ziejewski. Biomechanical assessment of brain dynamic responses due to blast pressure waves. *Ann. Biomed. Eng*. 38:490–504, 2010.
[10]Champion, H. R., J. B. Holcomb, and L. A. Young. Injuries from explosions: physics, biophysics, pathology, and required research focus. *J. Trauma* 66:1468–1477, 2009.
[11]Cronin, D. S., C. P. Salisbury, J.-S. Binette, K. Williams, *et al*. Numerical modeling of blast loading to the head. Paper Presented at PASS, Brussels, Belgium, 2008.
[12]Elkin, B. S., and B. Morrison, III. Region-specific tolerance criteria for the living brain. *Stapp Car Crash J*. 51:127–138, 2007.
[13]Frey, B., S. Franz, A. Sheriff, A. Korn, *et al*. Hydrostatic pressure induced death of mammalian cells engages pathways related to apoptosis or necrosis. *Cell. Mol. Biol*. 50:459–467, 2004.
[14]Galford, J. E., and J. H. McElhaney. A viscoelastic study of scalp, brain, and dura. *J. Biomech*. 3:211–221, 1970.
[15]Gordon, C. C., T. Churchill, C. E. Clauser, B. Bradtmiller, *et al*. Anthropometric Survey of US Army Personnel: Methods and Summary Statistics. Natick, MA: U.S. Army Natick Research Design and Engineering Center, Natick/TR-89/044, 1989.
[16]Gross, A. G. A new theory on the dynamics of brain concussion and brain injury. *J. Neurosurg*. 15:548–561, 1958.
[17]Hallquist, J. O. LS-DYNA Keyword User's Manual. Livermore, CA: Livermore Software Technology Corporation, 2007.
[18]Herbert, E., S. Balibar, and F. Caupin. Cavitation pressure in water. *Phys. Rev E*. 74:041603, 2006.
[19]Holland, C. M., E. E. Smith, I. Csapo, M. E. Gurol, *et al*. Spatial distribution of white-matter hyperintensities in alzheimer disease, cerebral amyloid angiopathy, and healthy aging. *Stroke* 39:1127–1133, 2008.
[20]Hyde, D. W. Conwep 2.1.0.8, Conventional Weapons Effects Program. Vicksburg, MS: United States Army Corps of Engineers, 2004.
[21]Iremonger, M. J. Physics of detonation and blast waves. In: Scientific Foundations of Trauma, edited by G. J. Cooper, and *et al*. Oxford: Butterworth Heinemann, 1997, pp. 189–199.
[22]Kaster, T., I. Sack, and A. Samani. Measurement of the hyperelastic properties of ex vivo brain tissue slices. *J. Biomech*. 44:1158–1163, 2011.
[23]Kleiven, S., and W. N. Hardy. Correlation of an FE model of the human head with local brain motion-consequences for injury prediction. *Stapp Car Crash J*. 46:123–144, 2002.
[24]Lubock, P., and W. Goldsmith. Experimental cavitation studies in a model head-neck system. *J. Biomech*. 13:1041–1052, 1980.
[25]Lynnerup, N., J. G. Astrup, and B. Sejrsen. Thickness of the human cranial diploe in relation to age, sex and general body build. *Head Face Med*. 1:1–13, 2005.
[26]Mahmadi, K., S. Itoh, T. Hamada, N. Aquelet, *et al*. Numerical studies of wave generation using spiral detonating cord. *Mater. Sci. Forum* 465–466:439–444, 2004.
[27]Manas, P., and B. M. Mackey. Morphological and physiological changes induced by high hydrostatic pressure in exponential and stationary-phase cells of escherichia coli: relationship with cell death. *Appl. Environ. Microbiol*. 70:1545–1554, 2004.
[28]McElhaney, J. H. Dynamic response of bone and muscle tissue. *J. Appl. Phys*. 21:1231–1236, 1966.
[29]McElhaney, J. H., J. L. Fogle, J. W. Melvin, R. R. Haynes, *et al*. Mechanical properties on cranial bone. *J. Biomech*. 3:495–511, 1970.
[30]Moore, D. F., A. Jerusalem, M. Nyein, L. Noels, *et al*. Computational biology—modeling of primary blast effects on the central nervous system. *Neuroimage*. 47:T10–T20, 2009.
[31]Moore, D. F., R. A. Radovitzky, L. Shupenko, A. Klinoff, *et al*. Blast physics and central nervous system injury. *Future Neurol*. 3:243–250, 2008.
[32]Moss, W. C., M. J. King, and E. G. Blackman. Skull flexure from blast waves: a mechanism for brain injury with implications for helmet design. *Phys. Rev. Lett*. 103:108702, 2009.
[33]Nelson, T. J., T. Clark, E. T. Stedje-Larsen, C. T. Lewis, *et al*. Close proximity blast injury patterns from improvised explosive devices in Iraq: a report of 18 cases. *J. Trauma* 65:212–217, 2008.
[34]Nicolle, S., M. Lounis, and R. Willinger. Shear properties of brain tissue over a frequency range relevant for automotive impact situations: new experimental results. *Stapp Car Crash J*. 48:239–258, 2004.
[35]Nusholtz, G. S., B. Wylie, and L. G. Glascoe. Cavitation/boundary effects in a simple head impact model. *Aviat. Space Environ. Med*. 66:661–667, 1995.
[36]Nusholtz, G. S., E. B. Wylie, and L. G. Glascoe. Internal cavitation in simple head impact model. *J. Neurotrauma* 12:707–714, 1995.
[37]Nyein, M. K., A. M. Jason, L. Yu, C. M. Pita, *et al*. In silico investigation of intracranial blast mitigation with relevance to military traumatic brain injury. *Proc. Natl Acad. Sci. USA* 107:20703–20708, 2010.
[38]Okie, S. Traumatic brain injury in the war zone. *N. Engl J. Med*. 352:2043–2047, 2005.
[39]Owens, B. D., J. F. Kragh, Jr., J. C. Wenke, J. Macaitis, *et al*. Combat wounds in operation Iraqi freedom and operation enduring freedom. *J. Trauma* 64:295–299, 2008.
[40]Panzer, M. B., C. R. Bass, and B. S. Myers. Numerical study of the role of helmet protection in blast brain injury. Paper presented at PASS, Quebec City, QC, 2010.
[41]Panzer, M. B., B. S. Myers, and C. R. Bass. Mesh considerations for finite element blast modeling in biomechanics. *Comput. Methods Biomech*. 2012. doi:10.1080/10255842.2011.629615.
[42]Panzer, M. B., C. R. Bass, K. A. Rafaels, J. Shridharani, *et al*. Primary blast survival and injury risk assessment for repeated blast exposures. *J. Trauma*. 2012. doi:10.1097/TA.0b013e31821e8270.

[43]Prange, M. T., D. F. Meaney, and S. S. Margulies. Defining brain mechanical properties: effects of region, direction, and species. *Stapp Car Crash J*. 44:205–213, 2000.
[44]Rafaels, K. A. Blast brain injury risk. Doctoral dissertation, University of Virginia, Charlottesville, VA, 2011.
[45]Rafaels, K. A., C. R. Bass, R. S. Salzar, M. B. Panzer, *et al*. Survival risk assessment for primary blast exposures to the head. *J. Neurotrauma* 28:2319–2328, 2011.
[46]Richmond, D. R., J. T. Yelverton, E. R. Fletcher, and Y. Y. Phillips. Physical correlates of eardrum rupture. *Ann. Otol. Rhinol. Laryngol*. 140:35–41, 1989.
[47]Ruan, J. S., T. Khalil, and A. I. King. Human head dynamic response to side impact by finite element modeling. *J. Biomech. Eng*. 113:276–283, 1991.
[48]Sack, I., B. Beierbach, U. Hamhaber, D. Klatt, *et al*. Non invasive measurement of brain viscoelasticity using magnetic resonance elastography. *NMR Biomed*. 21:265–271, 2008.
[49]Schneiderman, A. I., E. R. Braver, and H. K. Kang. Understanding sequelae of injury mechanisms and mild traumatic brain injury incurred during the conflicts in Iraq and Afghanistan: persistent postconcussive symptoms and posttraumatic stress disorder. *Am. J. Epidemiol*. 167:1446–1452, 2008.
[50]Taylor, P. A., and C. C. Ford. Simulation of blast-induced early-time intracranial wave physics leading to traumatic brain injury. *J. Biomech. Eng*. 131:061007, 2009.
[51]Terrio, H., L. A. Brenner, B. J. Ivins, J. M. Cho, *et al*. Traumatic brain injury screening: preliminary findings in a US army brigade combat team. *J. Head Trauma Rehabil*. 24:14–23, 2009.
[52]Valk, P. E., and W. P. Dillon. Radiation injury of the brain. *Am. J. Neuroradiol*. 12:45–62, 1991.
[53]Warden, D. L. Military TBI during the Iraq and Afghanistan wars. *J. Head Trauma Rehabil*. 21:398, 2006.
[54]Wardlaw, A. and J. Goeller. Cavitation as a possible traumatic brain injury (TBI) damage mechanism. Paper presented, College Park, MD, 2010.
[55]Wilkins, M. L. Use of artificial viscosity in multidimensional fluid dynamic calculations. *J. Comput. Phys*. 36:281–303, 1980.
[56]Wood, G. W., M. B. Panzer, J. K. Shridharani, K. A. Matthews, et al. Attenuation of blast overpressure behind ballistic protective vest. Paper presented at PASS, Quebec City, QC, 2010.